

Supporting material: Arbitrary hybrid and higher-order Poincaré sphere beams generation by metasurfaces via a unified design framework

Section S1. Phase modulation principle of meta-atom

As shown in Fig. S1(a), the metasurface comprises an array of periodically placed meta-atoms on a flat silica substrate. The meta-atoms in a dielectric metasurface generally have a subwavelength scale. The phase modulation ability of a metasurface is achieved by the local phase delay induced by each meta-atom. The local phase delay could arise from the resonance, propagation, and geometry phases (i.e., the PB phase).

When the dielectric meta-atoms have a height (H) much smaller than the working wavelength (λ), metasurface phase manipulation is achieved based on resonance phases, like the Mie, FP, Fano, and BIC. However, metasurfaces based on the resonance phase can only work in a narrow bandwidth. Moreover, resonance-based metasurfaces cannot focus incoming light with a high numerical aperture (NA) because the resonance mode coupling between adjacent meta-atoms would lead to significant errors in the case of large phase gradients. The following will analyse the propagation phase, geometry phase, and their combination based on the transmission matrix method.

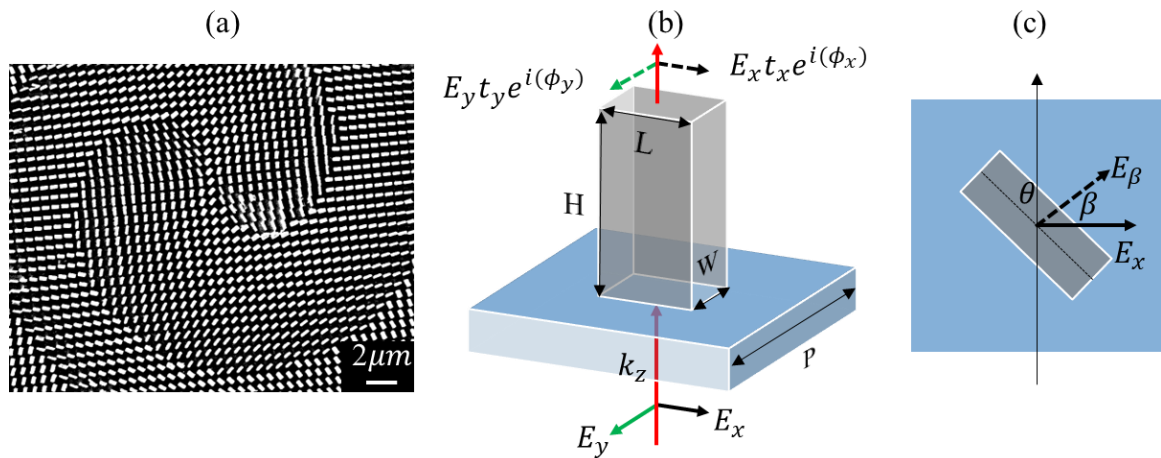


Fig. S1 (a) SEM image of a fabricated metasurface sample, (b) and (c) scheme of subwavelength meta-atom with a rectangle cross-section.

I Propagation phase of meta-atoms

The dielectric meta-atoms with a height H comparable to the working wavelength λ would introduce the polarization-independent propagation phase and the polarization-dependent propagation phase. The propagation phase is polarisation-independent when the meta-atoms have a rotationally symmetrical cross-section (e.g., square, circle). Otherwise, a polarization-dependent propagation phase would be introduced.

As shown in Fig. S1(b), the dielectric meta-atom can be treated as a truncated waveguide that has an effective refractive index n_{eff} . As the optical wave is confined inside the meta-atom, the propagation phase ϕ of the light wave propagating through the meta-atom can be defined as Eq. (S1),

$$\phi = \frac{2\pi}{\lambda} n_{eff} H \quad (S1)$$

As the n_{eff} is determined by the meta-atom's structural parameters (e.g., period P , width W , length L , and height H), material properties (e.g., refractive index n), the propagation phase ϕ can be tailored by varying the structural dimensions [Fig. S2(a)] and material selection. 2π phase coverage is necessary to achieve effective focusing of light waves. To achieve 2π phase coverage between the meta-atoms with the smallest and largest dimensions, the height H should meet Eq. (S2). The H is set as 800nm in this paper.

$$H > \frac{\lambda}{n-1} \quad (S2)$$

As the larger H would lead to a higher aspect ratio of the meta-atoms and increase the fabrication difficulty, we'd like to select the material with a larger refractive index n . The period P should be small enough to satisfy the Nyquist sampling criterion and reduce high-order diffraction [Eq. (S3)] for a target numerical aperture NA. The period P is optimised to be 650nm for realising highly focusing ($NA = 0.9$).

$$P < \frac{\lambda}{2*NA} \quad (S3)$$

Because the fabrication ability restricts the maximum filling factor, feature size, and highest aspect ratio of the meta-atoms, the fabrication of large NA metalens is quite challenging. Because of the high refraction index ($n = 3.45$), low absorption ($k \approx 0$) at a wavelength of 1550nm, and using the CMOS-compatible fabrication technique, this paper selects silicon as the meta-atom material.

As shown in Fig. S1(b) and S2(b), there is a phase difference $|\phi_x - \phi_y|$ between the propagation phases induced to the X-polarized light beam and Y-polarized light beam when the cross-section is a rectangle ($W \neq L$) because the X-polarized and Y-polarized light beams experience different structural dimensions. Therefore, the meta-atom works like a waveplate, and its function can be represented by a Jones matrix.

$$\begin{bmatrix} E_x^o \\ E_y^o \end{bmatrix} = \begin{bmatrix} \cos(\theta) & -\sin(\theta) \\ \sin(\theta) & \cos(\theta) \end{bmatrix} \begin{bmatrix} t_x e^{i\phi_x} & 0 \\ 0 & t_y e^{i\phi_y} \end{bmatrix} \begin{bmatrix} \cos(\theta) & \sin(\theta) \\ -\sin(\theta) & \cos(\theta) \end{bmatrix} \times \begin{bmatrix} E_x \\ E_y \end{bmatrix} \quad (S4)$$

Eq. (S4) shows that the transmitted light can be directly obtained at each lattice. In Eq. (S4), θ is the angle between the meta-atom length side and Y-axis, t_x (t_y) and ϕ_x (ϕ_y) are the transmission and propagation phases of the X-polarized (Y-polarized) light beam for $\theta = 0$, respectively. By optimising the meta-atom dimensions, both t_x and t_y can be meticulously crafted to achieve unity ($=1$) and $|\phi_x - \phi_y| = \pi$. As a result, equation (S4) can be simplified to Eq. (S5).

$$\begin{bmatrix} E_x^o \\ E_y^o \end{bmatrix} = e^{i\phi_x} \begin{bmatrix} \cos(2\theta) & \sin(2\theta) \\ \sin(2\theta) & -\cos(2\theta) \end{bmatrix} \times \begin{bmatrix} E_x \\ E_y \end{bmatrix} \quad (S5)$$

II Geometry phase of meta-atoms

When the incident light beam is LCP (i.e., $\begin{bmatrix} E_x \\ E_y \end{bmatrix} = |L\rangle = \begin{bmatrix} 1 \\ i \end{bmatrix}$), the transmitted light beam can be obtained as Eq. (S6), which means that the transmitted light beam is transferred to be RCP ($|R\rangle$) with a propagation phase of ϕ_x and a geometry phase of 2θ .

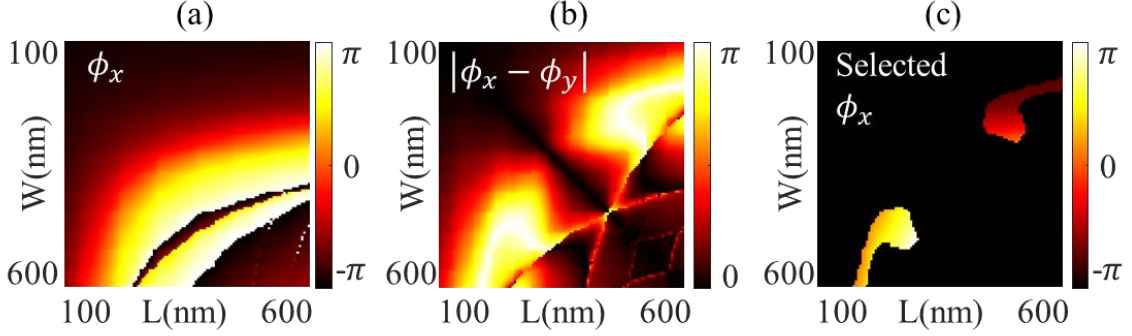


Fig. S2 (a) Propagation phase ϕ_x varies with the meta-atom's dimension, (b) Phase delay $|\phi_x - \phi_y|$ varies with meta-atom's dimension, (c) Selected meta-atoms library for achieving 2π phase coverage of ϕ_x and meeting the

requirements of $|\phi_x - \phi_y| = \pi$ and $t_x = t_y = 1$.

$$\begin{bmatrix} E_x^o \\ E_y^o \end{bmatrix} = ie^{i(\phi_x + 2\theta)} |R\rangle \quad (\text{S6})$$

When the incident light beam is RCP (i.e., $\begin{bmatrix} E_x \\ E_y \end{bmatrix} = |R\rangle = \begin{bmatrix} 1 \\ -i \end{bmatrix}$), the transmitted light beam can be obtained as Eq. (S7), which means that the transmitted light beam is transferred to be LCP with a propagation phase of ϕ_x and a geometry phase of -2θ .

$$\begin{bmatrix} E_x^o \\ E_y^o \end{bmatrix} = ie^{i(\phi_x - 2\theta)} |L\rangle \quad (\text{S7})$$

According to Eqs. (S6) and (S7), the geometry phase $\pm 2\theta$ imposed on the incoming LCP and RCP light beams is opposite; therefore, the geometry phase is a polarization-dependent phase. According to Eq. (2) and Fig. 1(a), arbitrary scalar beam ($\begin{bmatrix} E_x \\ E_y \end{bmatrix} = U$) is a sum of two orthogonal components, LCP and RCP. Substituting Eq. (2) into Eq. (S5), the transmitted light can be obtained as Eq. (S8).

$$\begin{bmatrix} E_x^o \\ E_y^o \end{bmatrix} = \tilde{A}_{RM} e^{i(\phi_x - 2\theta)} |L\rangle + \tilde{A}_{RN} e^{i(\phi_x + 2\theta)} |R\rangle = e^{i\phi_x} \{ \tilde{A}_{RM} e^{i(-2\theta)} |L\rangle + \tilde{A}_{RN} e^{i(2\theta)} |R\rangle \} \quad (\text{S8})$$

For a given meta-atom, the induced propagation phase ϕ_x is a constant value, which means that the phase carried by the transmitted light is only determined by the geometry phase $\pm 2\theta$. As shown in Fig. S2(c), we can vary meta-atoms dimension (i.e., L and W in Fig. S1) to realise 2π phase coverage. Based on the selected meta-atom library [Fig. S2(c)], polarization-dependent geometry phase $\pm 2\theta$ and polarization-independent propagation phase ϕ_x can be simultaneously utilised to manipulate the transmitted light wave phase.

III Simultaneous manipulation of local phase and polarisation

When the incident light beam is linear polarisation (LP) (i.e., $\begin{bmatrix} E_x \\ E_y \end{bmatrix} = \begin{bmatrix} \cos(\beta) \\ \sin(\beta) \end{bmatrix}$), the transmitted light beam can be obtained as Eq. (S9), which means that the transmitted light beam is linear polarisation with a propagation phase of ϕ_x . However, the polarisation direction of the transmitted light is rotated to $2\theta - \beta$ from the β . Equation (14) can simplify the explanation of the generation of the CVBs. Based on the meta-atom library [Fig. 3(c)], an incoming LP light beam's local phase profile and polarisation distribution can be simultaneously manipulated.

$$\begin{bmatrix} E_x^o \\ E_y^o \end{bmatrix} = e^{i\phi_x} \begin{bmatrix} \cos(2\theta - \beta) \\ \sin(2\theta - \beta) \end{bmatrix} \quad (\text{S9})$$

Section S2. Meta-atom's library

In general, the numerical simulation software (e.g., Lumerical FDTD solver, COMSOL, and CST) would be adopted to build up the meta-atom library. In this step, the first thing that should be considered is the polarization-dependence of light beam manipulation. Circular and square pillars are the typical choices for imposing the propagation phase if we want to manipulate the light polarisation independently. Meta-atoms are commonly chosen as elliptical and rectangle

nanofins to realise polarization-dependent manipulation. Moreover, elliptical and rectangle nanofins can be used to combine the propagation phase and geometry phase. As shown in Fig. S2, once the structure of the meta-atoms is confirmed, we can sweep the dimensions (e.g., H, P, W, L) to obtain 2π phase coverage with high transmission. In this paper, to manipulate the light beam via geometry phase and propagation phase induced by rectangle-shaped meta-atoms, a meta-atoms library [Fig. 2(b) in main context] was built up by selecting 9 meta-atoms from Fig. S2(c).

Section S3. Fabrication Flow

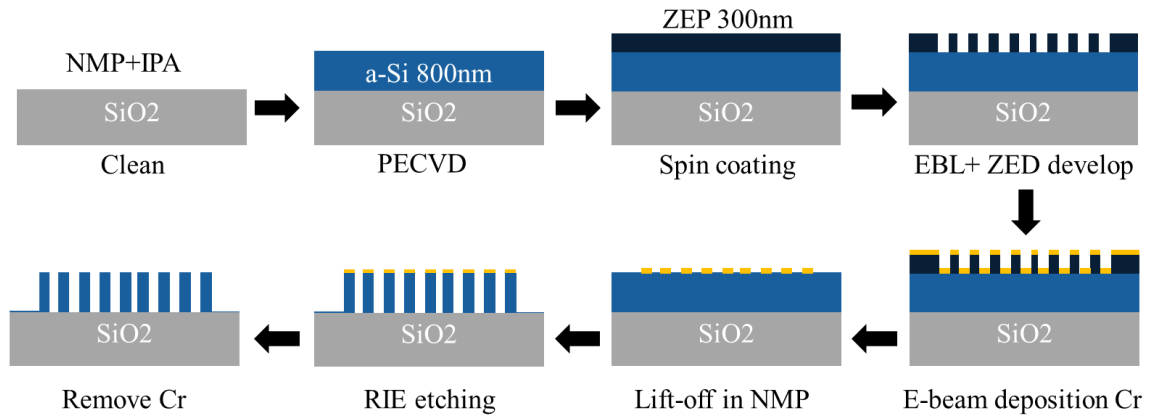


Fig. S3 Fabrication flow of the dielectric metasurface.

The 4 metasurface samples demonstrated in this research are fabricated in the cleanroom located at the University of Southampton following a CMOS-compatible process as shown in Fig. S3. The metasurfaces are fabricated on a double-side polished SiO_2 wafer. The wafer is first cleaned in NMP for 10 minutes and IPA for 10 minutes. Then, a layer of amorphous silicon (800nm in thickness) is deposited at a rate of 16nm/min via PECVD at 250°C. ZEP520A resist is spin coated on the wafer and baked on a hot plate for 3 minutes at 180°C. Subsequently, the metasurface's pattern is defined by the e-beam lithography (EBL) and development process in the ZED solution. As the hard mask, a 35nm-thick Cr layer is coated on the substrate by e-beam evaporation, followed by a lift-off in NMP. Consequently, the designed patterns are

transferred to the Cr layer, as shown in Fig. S3. Then, the wafer with the patterned Cr layer is dry etched by reactive ion etching (RIE) at a rate of 20nm/min. Finally, metasurface samples are obtained after removing the Cr layer via wet etching in the Cr etchant.

Section S4. Characterization setup

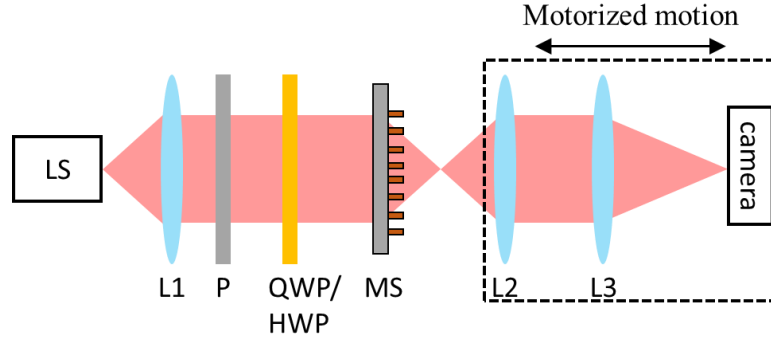


Fig. S4 Characterization setup of 4 dielectric metasurface samples. LS: 1550nm fibre laser (Thorlabs FPL1009); L1, fibre collimator (Thorlabs F810FC-1550); P1: polarizer; HWP: Half waveplate; QWP: Quarter waveplate; MS: metasurface sample; L2: objective lens; L3: tube lens (focal length = 200mm); Camera: InGaAs-based.

As shown in Fig. S4, a collimated 1550nm laser beam is incident to the rear surface of the metasurface sample. According to the Section 3.2 in main context, a pair of QWP and HWP is adopted to tune the incident laser beam's polarization state for manipulating the ongoing light field over a whole Poincaré sphere. Then, the ongoing light field is magnified and imaged to a camera via an infinity-corrected microscope. In addition, a polarizer is mounted between the L2 and L3 for measuring the X- and Y- polarization components, while the polarizer is removed from the setup for obtaining the total light field.